

Catalytic Silylation of Dinitrogen with a Dicobalt Complex

Randall B. Siedschlag,[†] Varinia Bernales,^{†,‡} Konstantinos D. Vogiatzis,^{†,‡} Nora Planas,^{†,‡} Laura J. Clouston,[†] Eckhard Bill,[§] Laura Gagliardi,^{*,†,‡} and Connie C. Lu^{*,†}

[†]Department of Chemistry and [‡]Supercomputing Institute & Chemical Theory Center, University of Minnesota, Minneapolis, Minnesota 55455-0431, United States

[§]Max Planck Institut für Chemische Energiekonversion, Stiftstraße 34-36, 45470 Mülheim an der Ruhr, Germany

S Supporting Information

ABSTRACT: A dicobalt complex catalyzes N₂ silylation with Me₃SiCl and KC₈ under 1 atm N₂ at ambient temperature. Tris(trimethylsilyl)amine is formed with an initial turnover rate of 1 N(TMS)₃/min, ultimately reaching a turnover number of ~200. The dicobalt species features a metal–metal interaction, which we postulate is important to its function. Although N₂ functionalization occurs at a single cobalt site, the second cobalt center modifies the electronics at the active site. Density functional calculations reveal that the Co–Co interaction evolves during the catalytic cycle: weakening upon N₂ binding, breaking with silylation of the metal-bound N₂ and reforming with expulsion of [N₂(SiMe₃)₃][−].

The N–Si bond has long been recognized as a useful linkage in organic synthesis for masking primary and secondary amines. Catalytic schemes to construct such bonds directly from N₂ are underdeveloped and could revolutionize the manufacturing of silylamines, which are increasingly important as industrial chemicals. For example, trisilylamines are used to fabricate silicon-nitride semiconductors in front-end electronic applications, and Si–N based polymers are incorporated into ceramic materials to impart thermal resistance.¹ Developing N₂ silylation catalysts² also complements ongoing research in N₂ fixation to ammonia, as they share the challenge of functionalizing N₂, a molecule that is both thermodynamically stable and kinetically inert, in an efficient and selective manner.³

A known catalyst for N₂ silylation is Mo(depf)₂(N₂)₂ (depf = 1,1'-bis(diethylphosphino)ferrocene), which produces N-(SiMe₃)₃ from N₂ (1 atm), Me₃SiCl, and Na_(s), with a turnover number (TON) of 150.^{2d} Efforts to surpass the Mo catalyst with a first-row transition metal have met with limited success.^{2b} A survey of iron coordination complexes showed subdued TONs, attaining a maximum of 34.^{2e,g} We report a dicobalt catalyst that achieves relatively high TON of N(SiMe₃)₃ at 299 K. The catalyst features a hemilabile metal–metal interaction, which is an unusual hallmark in catalytic N₂ functionalization.^{3g,4}

The precatalyst, Co₂L (1) comprises a (Co₂)³⁺ core within the trisphosphino(triamido)amine ligand (L^{3−}) framework (Figure 1, SI).⁵ Under N₂, the cyclic voltammogram of 1 showed two one-electron transfer processes at −2.11 and −2.54 V (vs Fc⁺/Fc, SI Figure 6). The first reduction is irreversible with Δ*E*_p of 0.4 V and an *i*_{pc}/*i*_{pa} ratio of 0.64. The electrochemical behavior is consistent with an ECE mechanism, where the chemical reaction

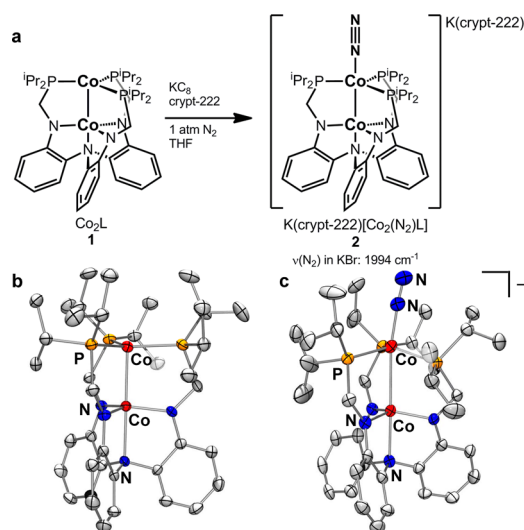


Figure 1. (a) Reduction of Co₂L (1) to generate K(crypt-222)-[Co₂(N₂)L] (2). (b,c) Molecular structures of 1 and 2, respectively, shown with 50% thermal ellipsoids. Hydrogen atoms (and counterion for 2) were removed for clarity.

(C) following the first electron transfer (E) is most likely dinitrogen binding.⁶ Indeed, reduction of 1 with 1 equiv KC₈ in the presence of N₂ and 2.2.2-cryptand (abbreviated as crypt-222) led to the isolation of K(crypt-222)[Co₂(N₂)L] (2) containing an end-on N₂ ligand (Figure 1). Infrared spectroscopy of 2 revealed an N–N stretching frequency of 1994 cm^{−1}, which is consistent with slight weakening of the N₂ triple bond.⁷

The molecular structures of 1 and 2 are shown in Figure 1b,c, respectively (SI Tables 1–2). The Co–Co bond distance elongates substantially from 2.32 to 2.68 Å upon reduction of Co₂³⁺ 1 to Co₂²⁺ 2. As the sum of the metallic radii of two cobalt atoms is 2.314 Å, the former is consistent with a Co–Co single bond, while the latter is a weak Co–Co interaction.⁸ The magnetic susceptibilities of 1 and 2 were measured from 2 to 290 K and are consistent with *S* = 5/2 and *S* = 1 ground states, respectively (SI Figures 9–11). The effective magnetic moment for sextet 1 decreases slightly from 6.1 to 5.8 μ_B from 50 to 290 K. To fit the data, a two-spin model is needed with ferromagnetic coupling (*J* = 60 cm^{−1}) between Co(II), *S* = 3/2, and Co(I), *S* = 1, centers. The triplet state of 2 is energetically isolated, with a *g*-

Received: February 13, 2015

Published: March 23, 2015

value of 2.14 and a zero-field splitting of 42 cm^{-1} , and can formally arise from antiferromagnetic coupling between $S = 3/2$ Co(II) and $S = 1/2$ Co(0) spins.

Since the anionic dicobalt N_2 adduct is stable to vacuum, we postulated that **2** could mediate the catalytic reduction of dinitrogen by using **1** as the precatalyst. Complex **1** was tested in catalytic N_2 silylation using a large excess of Me_3SiCl and reductant, KC_8 , under an atmosphere of N_2 . Standard catalytic conditions use a low catalyst loading (0.13 mM, 0.05 mol %) at 299 K for 12 h in THF. Under these conditions, **1** generated $\text{N}(\text{SiMe}_3)_3$ in 30% yield, with a TON of 195 ± 25 (Table 1).

Table 1. Reaction of N_2 (1 atm), Me_3SiCl (10.5 mmol), and KC_8 (10.4 mmol) Using Different Cobalt Precatalysts (5.27 μmol , 0.13 mM) in 40 mL THF at 299 K for 12 h

1 atm $\text{N}_2(\text{g})$ + 2000 $\text{Me}_3\text{SiCl}(\text{l})$ + 2000 $\text{KC}_8(\text{s})$		precatalyst (0.05 mol%) THF rt, 12 h	$\text{N}(\text{SiMe}_3)_3$	
entry	precatalyst	% yield ^a	TON ^b	
1	Co_2L (1)	30	195 ± 25	
2	$\text{K}(\text{crypt-222})[\text{Co}_2(\text{N}_2)\text{L}]$ (2)	27	178 ± 37	
3	$\text{Co}(\text{N}_2)\text{ALL}$	4	30 ± 9	
4	CoCl_2	1	6 ± 2	
5	$\text{Co}(\text{PPh}_3)_3\text{Cl}$	7	44 ± 11	
6	$\text{CoCl}_2 + 3 \text{PMe}_3$	13	86 ± 6	
7	$\text{CoCl}_2 + 3 \text{PMe}(i\text{-Pr})_2$	14	94 ± 19	
8	$2 \text{CoCl}_2 + \text{LH}_3$	25	172 ± 16	
9	$\text{CoCl}_2 + \text{LH}_3$	16	103 ± 20	
10	Co nanopowder ^c	0	0	

^a% yield (avg of 3 trials) is calculated for $\text{N}(\text{SiMe}_3)_3$ relative to Me_3SiCl . Amine was worked up and quantified by GC-MS (see SI).

^bTON (avg of 3 trials) = $[\text{N}(\text{SiMe}_3)_3]/[\text{precatalyst}]$. ^cCo nanopowder (carbon-coated, <50 nm particle size).

Based on the TON, **1** is one of the most active N_2 silylation catalysts, with comparable activity to $\text{Mo}(\text{deph})_2(\text{N}_2)_2$. Besides the desired product, $\text{N}(\text{SiMe}_3)_3$, other side-products are typically formed under these conditions, including $\text{Me}_3\text{SiSiMe}_3$, and mono- and bis-silylated THF, i.e., $\text{Me}_3\text{SiO}(\text{CH}_2)_3\text{CH}_2\text{R}$, where $\text{R} = \text{H}$ or SiMe_3 . The latter two byproducts can be suppressed by performing the catalysis in DME, but the TON for $\text{N}(\text{SiMe}_3)_3$ is slightly lower at 140 ± 9 (SI Table 5). Complex **2** was also catalytically competent and gave an identical TON as **1** (entry 2).

To test catalyst robustness, we performed two consecutive catalytic cycles using a 0.16 mM solution of **1**. In each cycle, Me_3SiCl and KC_8 (2000 equiv each) were added, and the reaction stirred for 12 h. The overall TON was 320 ± 18 . If the first cycle generates TON 195, then ~65% of the activity was retained in the second cycle (SI Table 5). We tested an isostructural Co–Al compound, $\text{Co}(\text{N}_2)\text{ALL}$, to gauge the effect of the supporting metal.⁹ Under standard conditions, $\text{Co}(\text{N}_2)\text{ALL}$ produced substantially less amine with a TON of 30 ± 9 (entry 3).

The catalytic functionalization of N_2 by cobalt complexes is unconventional, though low-valent cobalt complexes are known to bind N_2 .¹⁰ To investigate whether simple cobalt complexes can perform N_2 silylation, we screened some cobalt precursors (Table 1, entries 4–7). Even CoCl_2 is catalytic, although its activity is limited to a few turnovers (entry 4).^{2b} The Co(I) complex, $\text{CoCl}(\text{PPh}_3)_3$, is modestly active, with a TON of 44 ± 11 (entry 5). Increasing the Lewis basicity of the phosphine ligands dramatically raises the yield of $\text{N}(\text{SiMe}_3)_3$, and the TONs

reach ~100 for the trialkylphosphines, PMe_3 and $i\text{-Pr}_2\text{PMe}$ (entries 6–7). While the ligand (LH_3) does not generate any amine under standard catalytic conditions, mixing the ligand with two equivalents of CoCl_2 is as effective as **1** (entry 8). Of note, a 1:1 ratio of the ligand to CoCl_2 halves the TON relative to **1** (entry 9). Finally, the only cobalt precursor that did not generate any detectable amine was cobalt nanopowder (entry 10).

Catalytic N_2 functionalization can be highly sensitive to the reductant.^{2c,d,3e–g} Thus, we investigated catalysis by **1** with various alkali metals: $\text{Li}(\text{s})$, $\text{Na}(\text{s})$, and $\text{K}(\text{s})$. Using alkali metals significantly depressed the yield of $\text{N}(\text{SiMe}_3)_3$ (Table 2, entries 1–3). However, by prolonging the reaction time with $\text{K}(\text{s})$ from 12 to 95 h, the TON increases to 135 ± 29 (entry 4).

Table 2. Variation of Reductants or Additives with Complex **1 under Standard Catalytic Conditions (see Table 1)**

entry	reductant	% yield ^a	TON ^a
1	$\text{Li}(\text{s})$	3	19 ± 6
2	$\text{Na}(\text{s})$	1	7 ± 5
3	$\text{K}(\text{s})$	4	29 ± 3
4	$\text{K}(\text{s})$ ($t = 95 \text{ h}$)	21	135 ± 29
entry	additive ^b	% yield ^a	TON ^a
5	PMe_3	27	178 ± 4
6	$t\text{-BuNC}$	18	120 ± 13

^aCalculation of % yield and TON is the same as for data in Table 1.

^bAdditives are exogenous ligands. KC_8 is the reductant.

A difficult problem in catalysis is pinpointing the speciation of the active species, whether it be homogeneous or heterogeneous.¹¹ Though cobalt nanoparticles (NPs) were inactive for N_2 silylation, the elusive nature of active species and the ambiguity surrounding any single speciation tests prompted us to investigate this problem. To this end, we have probed the speciation of the catalyst through selective poisoning, a filtration test, initial rate studies, and *in operando* studies.

Since catalytic NPs have a smaller fraction of active metal sites relative to the bulk metal, they are readily poisoned by substoichiometric, exogenous ligands (per metal). For late metal NPs, phosphine ligands can be effective poisons.¹¹ In contrast, homogeneous metal catalysts require at least 1 equiv of phosphine to inhibit activity. The addition of 1 equiv PMe_3 per **1** effected no change in TON (Table 2, entry 5). The use of a π -acceptor ligand, $t\text{-BuNC}$, however, did lower the TON to 120 ± 13 , but the preservation of significant activity argues against a heterogeneous catalyst.

We also conducted a filtration test, whereby soluble and insoluble fractions are separated by filtration and then independently assayed for catalytic activity. In our variation of this test, one catalytic cycle is completed prior to filtering through graphite (SI Figure 13). The resultant filtrate is split into two equal parts, so that one half serves to exactly quantify the amine formed in the first cycle, TON 166.¹² The resultant precipitate and the other filtrate half are tested in a second catalytic cycle. If the active species is insoluble, then the overall TON will be ~166 for both the precipitate and the filtrate, as the latter carries the amine generated in the first cycle. However, if the active species is soluble, then the overall TON for the filtrate will double (for precipitate, TON 0). The overall TON for the filtrate was 316 versus 30 for the precipitate. Hence, the active species is soluble.

Although insoluble aggregates are discredited as active species, cobalt nanoclusters, by virtue of their smaller size, can be soluble and more challenging to detect or to exclude. Formation of active

nanoclusters may manifest in an induction period and/or irreproducible kinetic data. Initial rate experiments were conducted to determine the reaction order with respect to **1**. Amine formation was monitored by sampling the reaction mixture at discrete time points ($t = 2, 5, 10, 15,$ and 20 min). Per sample, the amount of $\text{N}(\text{SiMe}_3)_3$ was determined by converting $\text{N}(\text{SiMe}_3)_3$ into NH_4Cl with acid and then quantifying the ammonium by the indophenol method (SI).¹³ Rates of $\text{N}(\text{SiMe}_3)_3$ production were measured at four different concentrations of **1** (0.026, 0.13, 0.32, and 0.65 mM), and the initial rates show a pseudo-first-order dependence on catalyst concentration (Figure 2). The linear dependence of initial rates

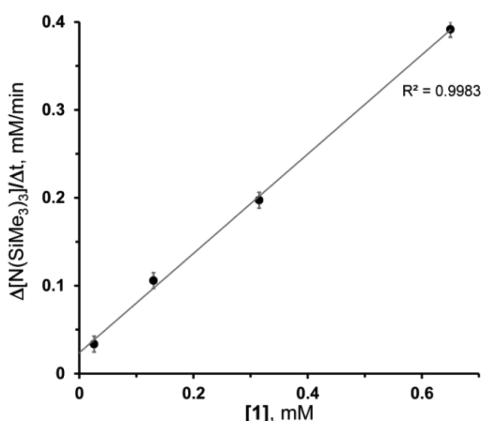


Figure 2. Plot of initial rates ($\Delta[\text{N}(\text{SiMe}_3)_3]/\Delta t$, mM min^{-1}) versus **1** (0.026–0.65 mM) in reactions with N_2 (1 atm), Me_3SiCl (21.3 mmol), and KC_8 (20.7 mmol).

on **1**, as well as the absence of a lag period, is consistent with a well-behaved homogeneous catalyst. We can approximate a turnover frequency of one $\text{N}(\text{SiMe}_3)_3$ molecule per minute.¹⁴

In operando studies were conducted to assess whether the active species is truly bimetallic. Complex **1** was mixed with a small excess of Me_3SiCl and KC_8 (10 equiv) under N_2 in $\text{THF-}d_8$ for 90 min. $^1\text{H NMR}$ analysis showed the presence of $\text{N}(\text{SiMe}_3)_3$ and 3 paramagnetic species, one of which is complex **2** (SI Figure 18a,b). If the reaction is quenched with a drop of CD_2Cl_2 , then only one paramagnetic species is observed, namely $\text{Co}_2(\text{Cl})\text{L}$. These observations are consistent with bimetallic active species.

Theoretical calculations were performed to gain insight into the catalytic mechanism and the electronic structures of **1** and **2**

(SI). The precatalyst, Co_2L , and potential active species, $[\text{Co}_2\text{L}]^-$ (**A**) and $[\text{Co}_2(\text{N}_2)\text{L}]^-$ (**B**), were found to have spin ground-states of $S = 5/2, 2,$ and $1,$ respectively. The ground states of Co_2L and **B** match that of their experimental counterparts, **1** and **2**. In all three structures, the Co–Co interaction is weak: the only delocalized molecular orbitals are $(\sigma)^2$ and $(\sigma^*)^1$, and their occupancies predict a bond order of 0.5. The precatalyst, Co_2L , contains an $S = 3/2$ $\text{Co}_\text{N}(\text{II})$ and $S = 1$ $\text{Co}_\text{P}(\text{I})$ (where Co_N and Co_P denote the Co sites in the N_3 - and P_3 -plane, respectively), in agreement with the magnetic data. In the “naked” anion, **A**, Co_P is reduced to $S = 1/2$ $\text{Co}_\text{P}(0)$, while the $S = 3/2$ $\text{Co}_\text{N}(\text{II})$ center remains unchanged. One effect of N_2 -binding (**A** \rightarrow **B**) is to change the nature of the magnetic coupling, leading to a lower overall spin state.

A catalytic mechanism and its energy profile are presented in Figure 3 (SI Figure 22). As proposed previously,^{2a,d} the SiMe_3 radical is the active silyl reagent under reducing conditions. The overall mechanism begins with N_2 -binding (**A** \rightarrow **B**), followed by three sequential additions of $\cdot\text{SiMe}_3$ to the N_2 ligand, and then expulsion of $[\text{N}_2(\text{SiMe}_3)_3]^-$ to regenerate Co_2L . It has been calculated that $[\text{N}_2(\text{SiMe}_3)_3]^-$ converts spontaneously to two $\text{N}(\text{SiMe}_3)_3$ via an uncatalyzed pathway.^{2d} Likewise, the Co_2L is easily reduced to **A** with KC_8 , closing the catalytic cycle. Alternative pathways, e.g. via a dicobalt nitride intermediate, were ruled out due to high activation barriers (SI Figure 23).

The notable section of the catalytic cycle is the cobalt-mediated reduction of N_2 by a total of four electrons to $[\text{N}_2(\text{SiMe}_3)_3]^-$. The three $\cdot\text{SiMe}_3$ equivalents add to the cobalt-bound N_2 in a distal–distal–proximal sequence, which is similar to the DFT-calculated mechanism for $\text{Mo}(\text{depf})_2(\text{N}_2)_2$.^{2d} The first $\cdot\text{SiMe}_3$ reacts with **B** to form the silyldiazenido(1-) intermediate **C**, with a barrier of 8.6 kcal/mol. The second addition of $\cdot\text{SiMe}_3$ generates the disilylhydrazido(2-) species **D**, with $\Delta G^\ddagger = 16.2$ kcal/mol, making this the rate-determining step. **D** then undergoes an exergonic dissociation of one phosphine donor, presumably to lessen the steric repulsion between the phosphine substituents and the disilylhydrazido ligand to give intermediate **D***, where the asterisk denotes one dangling phosphine arm. The third $\cdot\text{SiMe}_3$ preferentially attacks the proximal N atom, to form trisilylhydrazido **E*** with a low ΔG^\ddagger of 4.5 kcal/mol. Finally, phosphine association expels $[\text{N}_2(\text{SiMe}_3)_3]^-$ and regenerates Co_2L . No transition state could be found for this step (**E*** \rightarrow Co_2L), so we presume that this step is essentially barrierless.^{2d} Notably, the $\text{Co}\cdots\text{Co}$ distance changes dramatically in this elementary step, from 3.547 Å in **E*** to 2.522 Å in Co_2L , whereby

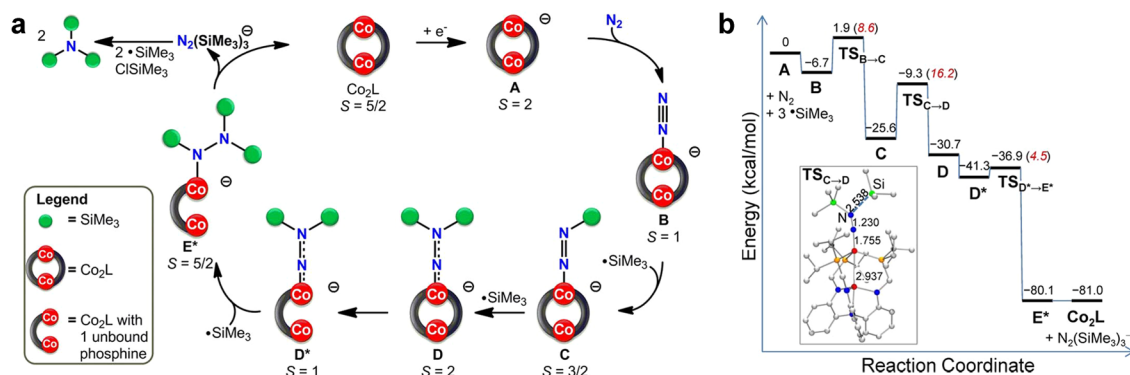


Figure 3. (a) DFT-calculated mechanism for the dicobalt-mediated silylation of N_2 . Intermediates with a dangling phosphine are labeled with an asterisk, e.g., **D***. (b) Energy profile (kcal/mol) for the proposed mechanism with activation energies in red. Inset shows $\text{TS}_{\text{C}\rightarrow\text{D}}$, the transition-state structure between **C** and **D** with interatomic distances in Å.

formation of the Co–Co bond may assist in releasing the $[\text{N}_2(\text{SiMe}_3)_3]^-$ product.

Considering the bimetallic nature of the catalyst, it is intriguing to examine the role of the second cobalt, Co_N . The supporting metal clearly affects the overall catalysis, as substituting Co with Al yields an isostructural Co–Al bimetallic that is less active by 6.5 times. The Co oxidation states and the nature of the Co–M bonds are quite different between these two systems. For the Co–Al system, the $(\text{CoM})^{3+}$ and $(\text{CoM})^{2+}$ species are consistent with $\text{Co}(0)\text{Al}(\text{III})$ and $\text{Co}(-1)\text{Al}(\text{III})$,^{5a} whereas in dicobalt, they are better described as $\text{Co}(\text{I})\text{Co}(\text{II})$ and $\text{Co}(0)\text{Co}(\text{II})$. In $[\text{Co}(\text{N}_2)\text{Al}]^-$, a strong inverse dative bond is present, $\text{Co}(-1) \rightarrow \text{Al}(\text{III})$, whereas in $[\text{Co}_2(\text{N}_2)\text{L}]^-$, the cobalt centers are weakly interacting. The Lewis acidic $\text{Al}(\text{III})$ metalloligand suppresses the catalytic activity at Co, and this is consistent with the electronic trend that increasingly basic phosphine ligands increase TON (Table 1, entries 4–6). Hence, the supporting metal can effectively tune the electron density at the active cobalt center, where $\text{Al}(\text{III})$ and $\text{Co}(\text{II})$ represent two electronic extremes of a metalloligand.

Though Co_N is potentially redox-active, our calculations show that this is not the case here (SI Figure 24). In the mechanism, Co_P cycles between $\text{Co}(0)$ and $\text{Co}(\text{II})$ in discrete one-electron steps, while Co_N maintains a constant oxidation state of +2 and $S = 3/2$. Although the reducing equivalents are stored only at the active cobalt, Co_N plays a significant role in stabilizing various $\text{Co}_\text{P}(\text{N}_2(\text{SiMe}_3)_x)$ ($x = 0$ to 2) intermediates, similar to the postulated mechanism of Rh_2 -catalyzed diazo-transfer reactions.¹⁵ Indeed, the Co–Co interaction increasingly weakens as N_2 binds and is functionalized to disilylhydrazido **D**, wherein the metal–metal bond is fully cleaved (SI Table 11). In the final step, the release of trisilylhydrazide is concomitant with Co–Co and Co–P bond formations.

Our study demonstrates that cobalt compounds can be effective catalysts for N_2 functionalization to $\text{N}(\text{SiMe}_3)_3$. The dicobalt system gives high TON while operating at 299 K and at low-catalyst loading. Additional experiments support the homogeneity of the active species. The catalysis is nearly 7-fold faster using KC_8 as a reductant, relative to K metal, likely because of the larger surface area in the former. We further demonstrate an interesting bimetallic strategy to electronically tune the active center through variation of the supporting metal atom. The $\text{Co}(\text{II})$ metalloligand was critical to achieve high TONs, suggesting that the traditional mode of tuning activity through the ancillary ligands (phosphines) may have a more limited effect than changing an ancillary metal (Al for Co). In future research, we will explore this idea by developing an isostructural family of Co–M bimetallics for catalytic N_2 silylation, where the ancillary metal is systematically varied.

■ ASSOCIATED CONTENT

📄 Supporting Information

Experimental/theoretical methods and data are provided (CCDC 962873–962875). This material is available free of charge via the Internet at <http://pubs.acs.org>.

■ AUTHOR INFORMATION

Corresponding Authors

*gagliard@umn.edu

*clu@umn.edu

Notes

The authors declare no competing financial interest.

■ ACKNOWLEDGMENTS

The authors thank Dr. Maria Miranda and Prof. Bill Tolman for GC-MS access, Andreas Goebels for magnetic data, and Yuxuan Chen for DFT help. This work was supported as part of the Inorganometallic Catalyst Design Center, an EFRC funded by the DOE, Office of Basic Energy Sciences (DE-SC0012702). C.C.L. is a Sloan Fellow. R.B.S. was supported by an NSF graduate fellowship. XRD experiments were performed using a crystal diffractometer (NSF-MRI, CHE-1229400) under the direction of Dr. Vic Young, Jr.

■ REFERENCES

- (1) (a) Belyi, V. I.; Vasilyeva, L. L.; Ginkover, A. S.; Gritsenko, V. A.; Repinsky, S. M.; Sinita, S. P.; Smirnova, T. P.; Edelman, F. L. *Silicon Nitride in Electronics*; Elsevier: Amsterdam, 1998. (b) Riley, F. L. *J. Am. Ceram. Soc.* **2000**, *83*, 245. (c) Nishi, Y.; Doering, R. *Handbook of Semiconductor Manufacturing Technology*; Marcel Dekker, Inc.: New York, 2000.
- (2) (a) Komori, K.; Oshita, H.; Mizobe, Y.; Hidai, M. *J. Am. Chem. Soc.* **1989**, *111*, 1939. (b) Shiina, K. *J. Am. Chem. Soc.* **1972**, *94*, 9266. (c) Liao, Q.; Saffon-Merceron, N.; Mézailles, N. *Angew. Chem., Int. Ed.* **2014**, *53*, 14206. (d) Tanaka, H.; Sasada, A.; Kouno, T.; Yuki, M.; Miyake, Y.; Nakanishi, H.; Nishibayashi, Y.; Yoshizawa, K. *J. Am. Chem. Soc.* **2011**, *133*, 3498. (e) Yuki, M.; Tanaka, H.; Sasaki, K.; Miyake, Y.; Yoshizawa, K.; Nishibayashi, Y. *Nat. Commun.* **2012**, *3*, 1254. (f) Mori, M. *J. Organomet. Chem.* **2004**, *689*, 4210. (g) Ung, G.; Peters, J. C. *Angew. Chem. Int. Ed.* **2015**, *54*, 532.
- (3) (a) Hazari, N. *Chem. Soc. Rev.* **2010**, *39*, 4044. (b) Hoffman, B. M.; Lukoyanov, D.; Yang, Z.-Y.; Dean, D. R.; Seefeldt, L. C. *Chem. Rev.* **2014**, *114*, 4041. (c) Leigh, G. J. *Haber-Bosch and Other Industrial Processes*. In *Catalysts for Nitrogen Fixation*, Smith, B. E., Richards, R. L., Newton, W. E., Eds.; Kluwer Academic: Dordrecht, 2004; Vol. 1, pp 33. (d) Hidai, M. *Coord. Chem. Rev.* **1999**, *185–186*, 99. (e) Schrock, R. R. *Acc. Chem. Res.* **2005**, *38*, 955. (f) Arashiba, K.; Miyake, Y.; Nishibayashi, Y. *Nat. Chem.* **2011**, *3*, 120. (g) Anderson, J. S.; Rittle, J.; Peters, J. C. *Nature* **2013**, *501*, 84.
- (4) (a) Powers, T. M.; Betley, T. A. *J. Am. Chem. Soc.* **2013**, *135*, 12289. (b) Moret, M.-E.; Peters, J. C. *J. Am. Chem. Soc.* **2011**, *133*, 18118.
- (5) (a) Rudd, P. A.; Liu, S.; Gagliardi, L.; Young, V. G., Jr.; Lu, C. C. *J. Am. Chem. Soc.* **2011**, *133*, 20724. (b) Clouston, L. J.; Siedschlag, R. B.; Rudd, P. A.; Planas, N.; Hu, S.; Miller, A. D.; Gagliardi, L.; Lu, C. C. *J. Am. Chem. Soc.* **2013**, *135*, 13142.
- (6) Amatore, C.; Saveant, J. M. *J. Electroanal. Chem.* **1978**, *86*, 227.
- (7) Holland, P. L. *Dalton Trans.* **2010**, *39*, 5415.
- (8) Pauling, L. *J. Am. Chem. Soc.* **1947**, *69*, 542.
- (9) Rudd, P. A.; Planas, N.; Bill, E.; Gagliardi, L.; Lu, C. C. *Eur. J. Inorg. Chem.* **2013**, *2013*, 3898.
- (10) (a) Betley, T. A.; Peters, J. C. *J. Am. Chem. Soc.* **2003**, *125*, 10782. (b) Ding, K.; Pierpont, A. W.; Brennessel, W. W.; Lukat-Rodgers, G.; Rodgers, K. R.; Cundari, T. R.; Bill, E.; Holland, P. L. *J. Am. Chem. Soc.* **2009**, *131*, 9471. (c) Greenwood, B. P.; Forman, S. I.; Rowe, G. T.; Chen, C. H.; Foxman, B. M.; Thomas, C. M. *Inorg. Chem.* **2009**, *48*, 6251.
- (11) (a) Crabtree, R. H. *Chem. Rev.* **2012**, *112*, 1536. (b) Windegren, J. A.; Finke, R. G. *J. Mol. Catal. A: Chem.* **2003**, *198*, 317.
- (12) Using the same concentration with double the volume (80 mL), the split-filtrate fraction of 40 mL can be directly compared to Table 1.
- (13) Weatherburn, M. W. *Anal. Chem.* **1967**, *39*, 971.
- (14) We verified the TOF by working up a standard catalysis at $t = 1$ h. By GC-MS, TON = 74 (or TOF of 1.2 $\text{N}(\text{SiMe}_3)_3/\text{min}$).
- (15) (a) Padwa, A.; Snyder, J. P.; Curtis, E. A.; Sheehan, S. M.; Worsencroft, K. J.; Kappe, C. O. *J. Am. Chem. Soc.* **2000**, *122*, 8155. (b) Pirrung, M. C.; Liu, H.; Morehead, A. T., Jr. *J. Am. Chem. Soc.* **2002**, *124*, 1014.